Journal of Cleaner Production 280 (2021) 124808

Contents lists available at ScienceDirect

Journal of Cleaner Production

journal homepage: www.elsevier.com/locate/jclepro

Development of industrially viable geopolymers from treated petroleum fly ash

Mohammad A. Al-Ghouti [a, *], Yahya S. Al-Degs [b], Ayoup Ghrair [c], Mahmoud Ziedan [d], Hani Khoury [e], Jafar I. Abdelghani [b], Majeda Khraisheh [f]

[a] Department of Biological and Environmental Sciences, College of Arts and Sciences, Qatar University, State of Qatar, Doha. P.O. Box: 2713, Qatar
[b] Chemistry Department, Faculty of Science, Hashemite University, Al-Zarqa, Jordan
[c] Department of Water Resources and Environmental Management, Al-Balqa Applied University, Salt, Jordan
[d] Chemistry Department, Hussein Thermal Power Station, Al-Zarqa, Jordan
[e] Earth Sciences and Environment Department, University of Jordan, Amman, Jordan
[f] Department of Chemical Engineering, College of Engineering, Qatar University, State of Qatar, Doha. P.O. Box: 2713, Qatar

ARTICLE INFO

Article history:
Received 23 June 2020
Received in revised form
26 September 2020
Accepted 21 October 2020
Available online 26 October 2020

Handling Editor: Cecilia Maria Villas Bôas de Almeida

Keywords:
Petroleum fly ash
Solid waste
Waste management
Geopolymer
Waste stabilization

ABSTRACT

This paper investigates the development of stable geopolymers using petroleum fly ash with high compressive strength and water absorption to promote cleaner production, sustainability, and recycling of waste. The paper provided detailed characterizations of the petroleum fly ash, which involved the determination of the particle size diameter, density, surface area, pore-volume, mineralogical identification of recording X-ray diffraction pattern, X-ray fluorescence, Fourier transform infrared, thermogravimetric analysis, and scanning electron microscope. Moreover, metals leachability from the petroleum fly ash using different extracting agents, namely H_2SO_4, H_3PO_4, $(NH_4)_2SO_4$, NH_4NO_3, and $NH_4O_2CCO_2H$ was also considered. Five geopolymers were prepared using different amounts of petroleum fly ash to assess the influence of petroleum fly ash on the final performance of the prepared geopolymers. The results revealed that the petroleum fly ash was carbonaceous in nature and rich in vanadium oxide and nickel oxide with low in SiO_2 and Al_2O_3. Furthermore, it was found that petroleum fly ash has a low calcium level. The maximum extraction values were 15.6% for V and 55.6% for Ni using H_2SO_4. All the prepared geopolymers displayed high compressive strength for longer curing times, and the water absorption properties of all geopolymers were improved by incorporating more petroleum fly ash. Increasing the petroleum fly ash from 0 vol% to 61 vol% increased the water absorption value from 6.6 to 13.3 wt% for the samples collected after 28 days of curing. It was concluded that the petroleum fly ash did tend to form successful stable geopolymers with high compressive strength and water absorption.

1. Introduction

Over the past decade, fly ash (FA) has received great attention in various fields. Fly ash is an industrial by-product, a powdery gray residue that is derived from the combustion of coal, petroleum products, or other relative materials in thermal power plants at 1200–1700 °C. It is important to highlight that the chemical composition of the produced FA varies due to the nature of the combusted fuel (i.e., either coal or petroleum material). For instance, the composition of coal fly ash (CFA) has been extensively studied. Vassilev and Vassileva (2005) mentioned in a study that around 316 individual minerals and 188 mineral groups have already been identified in CFA. While Lanzerstofer (2010) mentioned some of the main components in CFA include Ca, Fe, Si, and Al, in addition to any toxic and trace metals, which either come with coal (i.e., crust origin) or other external sources. On the other hand, the research on petroleum fly ash (PFA) is rather limited and is mostly related to physical and chemical analysis of the collected ashes (Al-Ghouti et al., 2011; Al-Degs et al., 2014). It is worth mentioning, unlike CFA, the residual carbon level in PFA is very high and can reach up to 80% in dry basis (Abdel-latif, 2002), and are characterized by higher excess carbon content (50 in some cases) with extremely low contents of Si and Al oxides (Al-Ghouti et al., 2011). Furthermore, most of the metals found in the PFA

* Corresponding author.
E-mail addresses: mohammad.alghouti@qu.edu.qa (M.A. Al-Ghouti), ayoup.ghrair@bau.edu.jo (A. Ghrair).

https://doi.org/10.1016/j.jclepro.2020.124808

are non-process elements, the prominent one being V, Ni, and Mg. Detailed chemical and physical characterizations of the PFA was, however, not reported.

Fly ash is discarded as an environmentally hazardous material rather than being recognized for its beneficial use (Blissett and Rowson, 2012). Mostly, about 80% of FA fate is disposed of in landfills, which poses environmental concerns. According to Yunusa et al. (2012), about 65% of FA produced in power stations is disposed to the landfills and ash ponds. Emissions of FA and its accumulation have led to severe environmental consequences and disposal challenges. As there are various key mechanisms, namely volatilization, melting, decomposition, and oxidation that causes the release and movement of trace metals from FA into soil and water (Munawer, 2018). Furthermore, the leachability of these metals causes another risk to the environment. Fly ash disposal can contaminate the nearby soil, making it unfavorable for most crops (Tiwari et al., 2015). Therefore, it is important to utilize FA in beneficial uses instead of disposing it into the environment (Han et al., 2020). Studies have been drawn to the use of waste material to avoid environmental concerns (Ahmaruzzaman, 2010). There have been relative studies over FA potential applications and environmental relevance, including concrete production, embankments (usually for roads), waste stabilization and solidification, cement clinkers, stabilization amendments for soft soil, adsorbents, and more recently in geopolymers (Al-Degs et al., 2014).

Geopolymers (GPs) are inorganic polymers that are formed by the polycondensation reaction of specific waste material that contains aluminosilicate with alkalis. Geopolymerization process could occur by aluminosilicate raw material dissolution in alkali solutions, which cause the formation of aluminate and silicate monomers. Then, oligomers and GPs will be formed as shown in Fig. 1 (Singh and Middendorf, 2020). Furthermore, it is widely known that GPs can reduce CO_2 emissions by 80% and energy consumption by 60% when it used as an alternative to cement (Assi et al., 2018; Hu et al., 2018; Li et al., 2020; Ma et al., 2019; Zhao et al., 2020). Moreover, GPs are considered a sustainable cement alternative due to their ability in consuming large quantities of industrial wastes as well as in eliminating the raw material transportation costs (Uzzal Hossain et al., 2018; Khan et al., 2020b). Fly ash is commonly available and abundant waste in most countries as it is expected that the production of FA will increase by 2.6 by 2033. For example, China produces around 500 million tons each year, while 131 million tons are produced by the USA annually (Shang et al., 2018). Approximately 45% of the produced FA is being used for different purposes such as cement and concrete production. On the other hand, the rest is being disposed of in landfills and storage lagoons which is nor cost-efficient neither environmentally friendly. Fly ash is usually used to produce GPs since it is aluminosilicate waste, thus, for cleaner production of solid wastes, the preparation of green FA-geopolymer is highly recommended (Zhao et al., 2020). In comparison to PFA-based geopolymers, geopolymers prepared from CFA contain a higher percentage of SiO_2 and Al_2O_3 (Bohra et al., 2019). Besides, GPs have a low environmental impact and have various benefits as an industrial use such as (Tan et al., 2020): (i) resistance to permeability, high temperature, acid, and sulfate attacks; and (ii) excellent mechanical and adsorption properties.

Nevertheless, no industrial-scale application has yet been realized. Besides, the economic barriers have not been overcome due to high value and high-volume utilization of the industrial application of FA. Depending on the nature of FA, many inertization protocols are applied to reduce the harmful influence of FAs on the environments, namely chemical washings (Hong et al., 2000), stabilization/solidification technology, incineration, extraction immobilization with construction materials (Dias-Ferreira et al., 2003). Petroleum and its derivatives are a dominant commercial fuel for various countries. The application of oil shale for generating electricity in the future might be a national issue. The amount of generated PFA in local power stations is not known exactly, however, there is a constant rise in the generated PFA due to the growth rate of energy demand, which is a growing concern. Public agencies have concluded that FA should be treated prior to its discharge due to its toxic nature. In a study conducted earlier, the extraction and separation of V and Ni from PFA were investigated. It was found that V and Ni are the most abundant metals while the chemical analysis revealed that the metal separation was acceptable (Al-Ghouti et al., 2011; Al-Degs et al., 2014).

Regarding the management of sustainable raw materials, it is significant to recycle industrial waste such as PFA as much as possible as well as to develop new technologies that result in new added-value materials. Adopting green ideology and ecological practices to achieve economic and social advantages without compromising environmental sustainability are required (Khan et al., 2019). Khan et al. (2019) investigated the use of green ideology to solve macro-level social and environmental problems. It was suggested that logistics operations were positively and significantly correlated with per capita income, manufacturing value-added, and trade openness. Whereas, it was negatively associated with social and environmental problems. The application of green energy resources and green practices can mitigate negative effects on social and environmental sustainability (Khan et al., 2019).

Based on our knowledge, there are insufficient studies in the literature regarding the recycling and reusing of PFA to prepare PFA-based geopolymers. Therefore, the current work aims to utilize PFA instead of disposing of it as a waste by preparing stable GPs with high compressive strength and water absorption as well as to determine the best utilization for each prepared GPs. Furthermore, this study provides also detailed characterizations of the PFA, which involved the determination of the particle size diameter, density, surface area, pore-volume, and mineralogical identification of recording X-ray diffraction pattern. In addition to the physical, chemical, and mechanical properties of the PFA-based geopolymers as well as the chemical stability, compressive strength, and water absorption of the prepared GPs. Moreover, metals leachability from the PFA using different extracting agents was also considered to evaluate the environmental impact of the prepared GPs and their potential applications.

2. Materials and methods

2.1. Collection of the PFA sample

About 2 kg of the PFA sample was collected as coarse particles at different times from Al-Hussein power station of 210 MW located in Zarqa, Jordan. The sample was mixed thoroughly and homogenized; no physical treatment was performed before use. The density of the collected PFA was 0.381 g/mL.

2.2. Morphological, physical, and chemical properties of the PFA sample

The ultimate, proximate, chemical, and mineralogical analyses of the collected PFA were determined. The textural properties of the PFA were evaluated by scanning electron microscopy (SEM) (FEI INSPECT-F50-SEM/EDX, The Netherlands). Particle Size Analyzer (Microtrac Zetatrac, Microtrac, USA) was used to measure the particle size distribution of the PFA.

Various techniques and methods were used to study the chemical composition of the collected PFA, namely inductively coupled plasma-mass spectrometry (ICP-MS, Shimadzu ICPS-7510

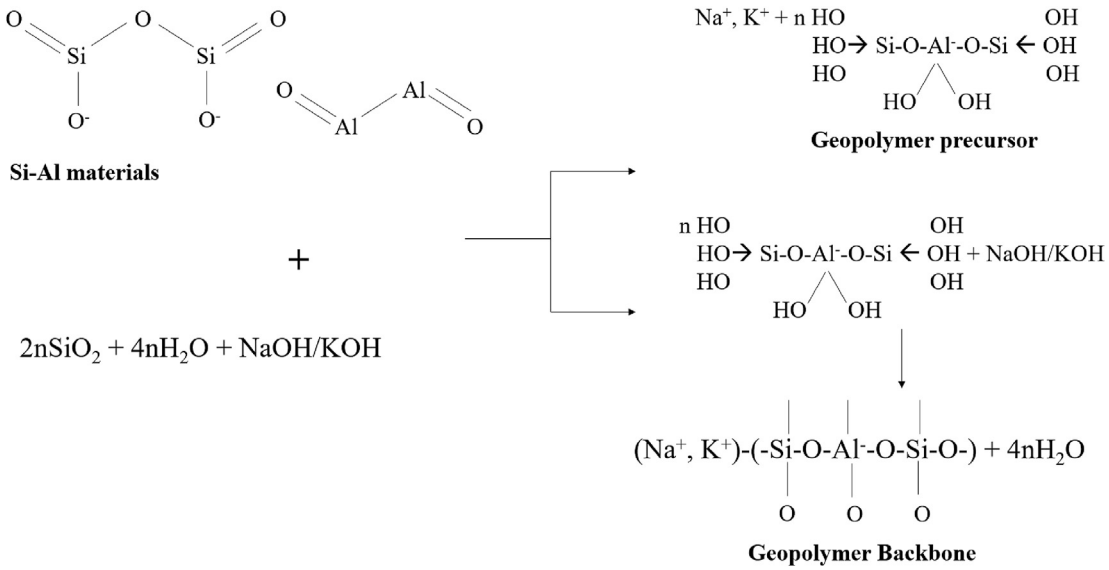

Fig. 1. Schematic illustration of geopolymer materials formation, modified from (Singh and Middendorf, 2020).

Sequential Plasma Spectrometer, Japan), X-ray diffraction (Shimadzu X-ray Diffractometer XRD-6000, Japan), Fourier transform infrared (FTIR-Perkin-Elmer Spectrophotometer RX I), thermogravimetric analysis (Mettler TGA/SDTA 851e thermos-balance) and X-ray fluorescence measurements (Shimadzu XRF-1800 Sequential X-Ray Fluorescence Spectrometer, Japan). The surface area of the sample was determined using nitrogen adsorption measurements (liquid nitrogen temperature, 77 K, Brunauer, Emmett, and Teller (BET) equation). Different extracting agents, prepared from H_2SO_4, H_3PO_4, $(NH_4)_2SO_4$, NH_4NO_3, and $NH_4O_2CCO_2H$, were tested for the metal extraction from PFA. The "liquid to solid" "L/S" ratio was maintained at 50.0 cm^3/g, using 1.0 M solution agitated for 24 h at 25 °C (±1 °C), and centrifuged (5000 rpm).

2.3. Physical and chemical properties of prepared PFA based-geopolymer

Natural clay (100% kaolinite, particle size 45 μm–63 μm, and plasticity limit 22%) was used for the preparation of five GPs containing variable amounts of the PFA (0%–42 wt%). The full description of the geopolymerization process was published in Al-Ghouti et al. (2011) and Al-Degs et al. (2014). In order to achieve high stable composites, a gentle stirring of the PFA with 100 g kaolinite and 16.6 M NaOH was performed. The resulted pastes of the GPs were then homogenized and molded immediately in a cylinder. The samples were then cured at 80 °C for over the period 1, 7, 14, and 28 days. The compressive strength and water absorption tests for the prepared geopolymers were conducted. For the assessment of the matrix stability of the prepared GPs, pH, and electrical conductivity measurements over the period 1–24 h were carried out for all GPs samples including PFA.

3. Results and discussions

3.1. Physicochemical characterization of the PFA

3.1.1. Morphological and chemical properties of the PFA

The loss of ignition (LOI) value of all particle size fractions was relatively high (30.4%–33.8%) indicating an incomplete combustion of the feed fuel. The high LOI value might also be useful in giving recommendations regarding the use of this ash for producing heat. However, this would only be possible after the removal of the inorganic matter. It is important to mention that the high LOI would affect the application of the ash in the cement industry since the recommended LOI value should not be more than 7% (Jones et al., 2006). As shown in Table 1, the PFA particles have an acceptable specific surface area (SSA). Furthermore, the results also indicated that the feed fuel was the main source of the elemental structure. It was found that the PFA consisted of a high amount of metals including vanadium oxide and nickel oxide. Furthermore, the produced PFA had the lowest percentage of Al_2O_3 and SiO_2 when compared to other ashes obtained from coal burning, which is an important factor as it determines the potential application of this ash. Generally, the total percentage of Al_2O_3 and SiO_2 in most of the ashes attained from coal-burning is within 70%–85% (Al-Ghouti et al., 2011), while Bohra et al. (2019) found that the CFA content of SiO_2 and Al_2O_3 is 39.18% and 22.64%, with a recommended ratio of 3.0–3.8 for higher strength (Komnitsas and Zaharaki, 2007). However, the results that were obtained from this study showed that both oxides added up to only 1.3%. The significant low percentage of both oxides could perhaps be due to the low content of Si and Al in the feed fuel. Kim and Prezzi (2008) mentioned in a study that FA could be categorized into Class C and F based on the AASHTO M 295 classification system. This classification is based on the CaO content, in which the Class C FA has ≥20% CaO, while Class F FA is generally low in CaO, which is ≤ 10%. The removal of iron oxides from ash has been reported to be a common practice toward certain applications. Furthermore, another standard for the classification of FA is the Canadian Standard (CAN/CSA-A3000-03). It classifies FA into 3 groups based on the calcium oxide percentage, namely class F, CI, and CH. The studied PFA is categorized under Class F as it contains calcium less than 8 wt%. PFA with low calcium is more preferable due to the less interference of calcium during the polymerization process as well as affecting the microstructure (Wattimena et al., 2017). Furthermore, Khan et al. (2020a) compared the durability of low-calcium fly ash-based geopolymer mortar (FA-GPm) with the sulfate resistant Portland cement mortars (SRPCm), which was estimated under two testing environments: natural sewer and 1.5% H_2SO_4 solution. The results illustrated that in terms of mass loss, compressive strength, dry bulk density, and surface disintegration, a greater deterioration was experienced by SRPCm in comparison to FA-GPm. On the other

Table 1
Different physicochemical characteristics of the collected PFA.

Particle size (μm)	Mass percentage (wt%)	Bulk density (g/mL)	Loss of ignition (LOI)	Specific surface area (SSA) (m^2/g)[a]
>106	13.3	0.355	36.4	0.16
63–106	44.3	0.381	38.2	0.19
45–63	23.4	0.421	34.8	0.26
<45	19.0	0.486	35.6	0.27

[a] Theoretical SSA = 6/(dp × density) for spherical particles. The dp is the particle diameter.

hand, in both testing conditions, the FA-GPm was visually intact in terms of corrosion depth, pH reduction, and neutralization depth. Moreover, it was suggested by the natural investigations of microbial induced concrete corrosion (MICC) that FA-GPm has better performance than SRPCm if used in plain concrete members or as a sacrificial coating material. This can be attributed to the resilience toward the surface disintegration. According to Zhou et al. (2019) low calcium FA geopolymer cannot be directly used as backfill grouting materials, thus adding a calcium source is an effective way to improve its fresh and mechanical properties. Calcium sources include soda residues could enhance the early strength and microstructure of low-calcium FA (Zhao et al., 2019).

Similarly, Vitolo et al. (2000) observed a low content of Si and Al (total 5.6%) in heavy fuel FAs. It can be concluded that the high amounts of SiO_2 and Al_2O_3 that are present in coal ashes could be due to the high content of Si and Al in the original coal. The large amounts of SiO_2 and Al_2O_3 in various ashes have been investigated for the application of FA in GPs and other construction materials (Pilehvar et al., 2018). In another study, Pires and Querol (2004) observed a very high level of MgO (13.12%) in fuel FA, which is usually not in the case of coal ashes. This perhaps can be due to high doses of Mg added to feed fuel (see Table 2) which is necessary for preventing deposits, reducing corrosions, and neutralizing acid that is produced at higher temperatures. The ash obtained from heavy fuel burning also had relatively high carbon content (34.6%) which seemingly is higher than the level in coal origin (Al-Degs et al., 2014). One of the reasons for the presence of sulfur-containing minerals could perhaps be due to the feed fuel, which could be made up of high sulfur content, thus while reacting with other elements at 1200°C sulfur might have formed various sulfur-containing minerals.

3.1.2. Levels of crust and anthropogenic metals in feed fuel and the PFA

Table 2 shows the concentration of both crust and anthropogenic metals in the feed fuel and the PFA. Crust metals (Al, Ca, Fe, Mg, Na, Si, and S) are originated from the earth's crust and fused with petroleum material during its creation, however, the anthropogenic metals are supposed to be added during the long processing steps of petroleum material. As evident from Table 2, all metals in the PFA were found in high quantity. Which concedes with other studies done previously. However, the only exception was for S where the level was reduced from 1.2% in the feed fuel to 585 mg/kg in the PFA. This perhaps can be due to the formation of SO_2 and SO_3 oxides while the remaining S might have reacted with other metals to form stable oxides, which agrees with the results obtained from XRD analysis. Metals enrichment in the PFA was determined by calculating the enrichment factor (EF). There are various procedures for the determination of EF (Kröppl et al., 2011). In this study, the EF was estimated for each element from equation (1),

$$EF = [M]_{PFA} \Big/ [M]_{fuel} \quad (1)$$

Table 2
Major and trace elements (crust and anthropogenic) in the feed fuel and the PFA (63 μm–106 μm) (dry basis analysis), as well as major oxides, proximate analysis, and mineral content.

Crust metals	Feed fuel	PFA	Enrichment factor[b]
Al	38.9 mg/kg	0.28 wt%	71
Ca	48.6 mg/kg	0.57 wt%	118
Fe	33.4 mg/kg	0.34 wt%	102
Mg	238.5 mg/kg	7.87 wt%	330
Na	111.4 mg/kg	2.40 wt%	215
Si	55.6 mg/kg	0.40 wt%	72
S	1.2 wt%	585 mg/kg	0.05
Anthropogenic metals			
Cr	5.6 mg/kg	146 mg/kg	26
Cu	3.5 mg/kg	92.5 mg/kg	26
Mo	5.3 mg/kg	85 mg/kg	24
Ni	103.2 mg/kg	0.71 wt%	69
Pb	3.4 mg/kg	7.8 mg/kg	2
V	112 mg/kg	3.1 wt%	277
Zn	6.8 mg/kg	247 mg/kg	36

Major oxides (wt%)		Proximate Analysis (wt%)		Mineral Content	
MgO	13.12	Moisture	1.62	$PbSO_4$	Major mineral
Fe_2O_3	4.92	Ash	37.2	$Mg_3V_2O_8$	Major mineral
Na_2O	3.24	Volatile matter	12.1	MgO	Minor mineral
Al_2O_3	0.52	Fixed carbon	34.6	Quartz	Trace mineral
SiO_2	0.86	Sulfur	0.06	Magnetite	Trace mineral
CaO	0.80	Total organic carbon	31.0		
		LOI	38.2		

where $[M]_{PFA}$ and $[M]_{fuel}$ stands for metal/element content (in mg/kg or wt.%) in the PFA and the feed fuel, respectively. For the curst metals, very high EFs were observed, for Mg (330) and Na (215), these values were higher in contrast to other metals in the feed fuel.

The formation of stable MgO at a high burning temperature (1200°C) was achieved, which was confirmed by the XRD analysis. For anthropogenic metals, the highest EF value was observed for V, which can be due to the formation of stable V oxides (as confirmed by XRD analysis), at the high temperature. The high levels of V and Ni were also reported in previous work (Al-Ghouti et al., 2011). It is also important to study the fractionation of the C atom as this element makes up to 86.3% of the feed fuel. The total content of C in the PFA is 34.6%, which reveals that 60% of C has been combusted (mainly as CO and CO_2 at 1200°C) while the rest of this element is distributed between PFA and bottom ash.

Furthermore, both CFA and PFA contain a high amount of toxic metals such as V, Ni, Mn, Pb, and Hg, which would be dangerous if directly discharged into the environment (Zhuang et al., 2016). A similar observation was reported by Shon et al. (2004), in which the V concentration of 6100 mg/kg was reported in PFA. In a study conducted by Al-Ghouti et al. (2011), extremely high levels of V (3200 mg/kg) and Ni (7100 mg/kg) were found in PFA. These ashes were obtained from the formal Al-Aqaba power station (Al-Aqaba, Jordan) that used diesel for power generation. It was concluded that V and Ni were present in a much lower amount in CFAs in contrast with PFA, which will give value that is more industrial for PFA after

performing extraction and separation procedure. This was explained due to the addition of earlier elements to the petroleum flue during the processing stages. Moreover, the presence of Mo was also present in a good amount (85 mg/kg - 720 mg/kg) in petroleum ashes in contrast to coal ashes.

3.1.3. Particle size distribution of the PFA particles

It is important to study the particle size range of the collected PFA as it gives a good understanding of the combustion process of the fuel. If the combustion process is successful, the PFA particle size should be between 0.2 μm and 90 μm. This is due to the complete transformation of mineral matter. However, particle size ranging between 90 μm and 300 μm often indicates poor combustion (Shirai et al., 2011). These large particles usually consist of char, partially combusted carbon matter with large dimensions. From the results obtained by Yu et al. (2015), about 44% of the ash particles were within 63 μm−106 μm range, while particles of size more than 106 μm were making up to 13.3%. Based on the earlier discussion (Al-Degs et al., 2014), the fuel-combustion process was more effective if the diameter of the collected FA particles were less than 106 μm. Since the current collected PFA was mostly between 63 μm −106 μm fraction, the characterization studies were carried out using this range. From the results, it could be inferred that the produced ash has a carbonaceous nature, which is obvious due to the high level of fixed carbon (34.6% for 63 μm−106 μm) coupled with a low bulk density of 0.381 g/mL. Furthermore, the particle size distribution of the PFA was assessed as it helps to understand the impact of the ash in the environment, particularly the atmosphere as well as to determine its appropriate industrial applications.

In this study, the following parameters were drawn: $dp_{<10\mu m}$, $dp_{<50\mu m}$, $dp_{<90\mu m}$, D_{10}, D_{50}, and D_{90}. The distribution analysis of the PFA agreed with the experimentally collected size range (63 μm−106 μm) where 99.5% of the particles have a diameter of less than 90 μm. Moreover, the particle diameter of PFA of dp less than 10 μm has been added to concrete to replace fine cement particles, however, the PFA of particle diameters less than 45 μm are employed as fillers in other construction materials or as adsorbents (Gisi et al., 2016). Based on that, the collected ash is applicable in construction materials or as adsorbents. Besides, with the fine particle size, the ashes used in construction materials should have high contents of Si and Al oxides, which were not found in this case. Having said that, the addition of ash of low Si/Al content to construction composites is a well-known inertization technique in order to get rid of unwanted toxic by-products (Hossaini et al., 2015).

It is worth mentioning that particle size analysis is often carried out if the particles have spherical shapes (Bray et al., 2013). However, such an assumption would be applied to particles of a rod, ellipse, or even irregularly shaped particles (Bray et al., 2013). The Arithmetic mean diameter (AMD) (70.2 μm) is much larger than the one observed for CFA obtained from power stations which can be attributed to the high content of inorganic matters (Al-Degs et al., 2014). The earlier authors reported very fine particle diameters and these variations in size distribution due to the different nature of the employed fuel at the station, which may include oil shale or coal. The particle size range of PFA fell within the range of atmospheric aerosols (0.001 μm−100 μm) (Foret et al., 2006). Accordingly, the PFA should not be discharged directly to the environment. This fine material could be lifted by the atmosphere; hence can cause health problems (Foret et al., 2006). The specific surface area of the PFA is 0.22 m^2/g and this value was estimated from AMD value (70.5 μm) and the bulk density of the ash (0.381 g/cm^3) and assuming a spherical shape for the particles (Foret et al., 2006).

3.1.4. Scanning electron microscopy and energy dispersive X-ray spectrometry (SEM/EDX)

Application of SEM is often carried out to understand the morphology of the surfaces at high magnifications, and when combined with EDX, it would be possible to find out the elements making up the surface (Al-Ghouti et al., 2012a). The recorded SEM micrographs (at different magnification power) are shown in Fig. 2 (A-D).

The process of fuel burning was inefficient or incomplete as indicated by the relatively high LOI value. This would end up with a wide distribution of char and porous carbonaceous materials with different dimensions. During this complex burning process, the formation of agglomerate and crystalline materials is also possible. The carbonaceous nature of the materials would be deduced from the porous spherical particles as viewed in Fig. 2, which is expected due to the level of carbon in the sample. The chemical analysis revealed the presence of a good amount of Mg, Na, Fe, and Si oxides and this confirmed by the detection of solid particles of irregular shapes with sizes less than 10 μm to higher than 100 μm. The particles of carbonaceous material have a porous structure while inorganic surfaces appear as solid/crystalline particles with small particle diameter. It is highly possible that condensation of C and S compounds that form at high temperatures would be happening. The presence of crystalline x40,000 magnifications (Fig. 1D) where oxides (mainly oxides of V, Ni, Fe, and S) of needle-like and plate-like structures could be viewed. The EDX indicated the presence of C, O, V, Na, Mg, and S within the matrix of the PFA. The absence of Al, Ca, Fe, and Si for the EDX spectra would be attributed to the condensation of C, Na, and Mg oxides and sulfides over the oxides of the earlier elements. The formation of sulfide complexes has been reported in the XRD (Fig. 1E). Based on the SEM analysis, the industrial application of this ash could be optimized as fillers, water absorption, and solid adsorbent. While the spherical and fine particles of the ash would give good application in concrete and other construction materials.

3.1.5. Mineralogical analysis by XRD

For obtaining detailed information regarding the mineralogical composition of the PFA, an XRD was obtained (Fig. 2E). For phase identification, the diffraction data were analyzed with the aid of the PC-Identity and the International Centre for Diffraction Data (ICDD) database. The results revealed that the major minerals were $PbSO_4$, $Mg_3V_2O_8$, and MgO. Quartz and magnetite were found as minor minerals. Carbon was also detected in a large fraction, which reinforces the presence of carbon in the sample. The XRD analysis confirmed that V and S, which were present in feed fuel, reacted with Pb and Mg to form stable oxides in the PFA. Even though the crystallinity (which refers to the degree of structural order in the ash) was not estimated. The material seems to be of low crystallinity, which was indicated by the large amounts of carbonaceous porous particles, which was also observed from the SEM analysis. Based on the XRD results, it can be said that the ash is a good source of V and could be extracted by applying a suitable extraction/separation procedure. It is worth mentioning that Ni-complexes were not detected by the XRD while the chemical analysis indicated that V and Ni were present in quiet good amounts in the ash. The crystallinity ranges between 85% and 100%. The results also confirmed that the PFA was rich with carbon and sulfate with 80%−88% by mass.

3.1.6. Fourier transform infrared (FTIR)

Fig. 2F shows the FTIR spectrum of the PFA. It shows the chemical changes that might have occurred due to combustion and how this might have led to the formation of various functional groups in the PFA. The main FTIR peaks were found at 3650 cm^{-1},

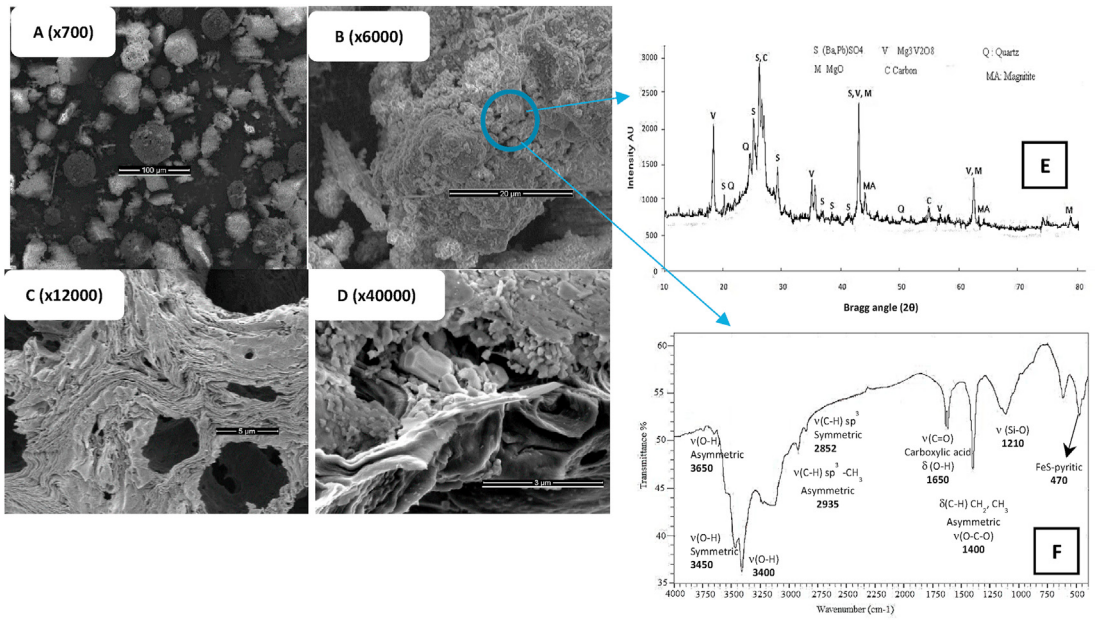

Fig. 2. A–D: SEM micrographs of the PFA at different magnifications (700–40,000), E. X-ray diffraction, and F. FTIR spectrum of the PFA (Al-Ghouti et al., 2011; Al-Degs et al., 2014).

3450 cm^{-1}, 3400 cm^{-1}, 2935 cm^{-1}, 2852 cm^{-1}, 1685 cm^{-1}, 1650 cm^{-1}, 1400 cm^{-1}, 1210 cm^{-1}, 630 cm^{-1}, and 470 cm^{-1}. The peaks that appeared at 3650 cm^{-1}, 3450 cm^{-1}, 3400 cm^{-1} are attributed to the vibrational frequencies of the O–H bond present in H_2O. The incomplete combustion of feed fuel was not accomplished; this was confirmed by the peaks 2935 cm^{-1} and 2852 cm^{-1} that are attributed to CH_3 asymmetric and CH_2 symmetric stretching vibrations, respectively (Al-Ghouti et al., 2012a). The main peaks present in the feed fuel are mostly related to C–H bond (sp^3 CH_3 (asymmetric), sp^2 CH_2 (olefinic), sp^3 CH_2 (asymmetric), sp^3 CH, sp^3 CH_3 (symmetric), and sp^3 CH_2 (symmetric)) which appeared at 2935 cm^{-1}, 2924 cm^{-1}, 2852 cm^{-1}, and 1458 cm^{-1}. However, the earlier peaks have low intensity indicating the small content of unburned fuel. The peaks positioned at 1650 cm^{-1} and 1400 cm^{-1} were owed to OH bending frequency in a carboxylic acid group, which would form upon fuel combustion at high temperatures. The characteristic peak was observed at 1210 cm^{-1} indicated the presence of Si–O bond stretching (the asymmetric stretching vibration of the TO4 tetrahedra, where T represents Si or Al), which was the only inorganic part noted. The formation of S-complexes at high temperatures was observed at 470 cm^{-1} which corresponds to FeS-pyritic bond (Sing, 2001).

3.1.7. N_2-adsorption tests

For an accurate evaluation of the porosity and surface area of the PFA, the nitrogen adsorption test was carried out. The recorded N_2-isotherm was type IV according to Gills classification (Sing, 2001), where a steep adsorption at a relative pressure of 0.9 was observed. The SSA was determined by the Brunauer-Emmett-Teller (BET) method and it was found to be 3.0 m^2/g, which is 15 times higher than the theoretical value (0.19 m^2/g, which would reflect the high porosity of PFA). N_2 adsorption data were analyzed by the Barret-Joyner-Halenda (BJH) method revealed the mesoporous structure of the PFA with a total pore volume of 0.02 cm^3/g with an average pore width of 22.2 nm. From the earlier results, the application of the PFA as adsorbent seems to be not practical where the total pore volume and the SSA are modest when compared to commercial activated carbon (Nunes and Guerreiro, 2011).

3.1.8. Thermogravimetric analysis

Thermogravimetric analysis (TGA) was employed to monitor the degradation behavior of the PFA. The recorded thermograms indicated the stability and its resistance to thermal degradation up to 340 °C. However, a notable mass loss (34%) was observed at 890 °C, which reflected the degradation of the organic matter of the PFA. Analysis of thermogravimetric data also revealed that moisture content is 2.6 wt% at 110 °C and the ash content was 38.0% at 900 °C while the fixed carbon was 33.3%. The results obtained by the TGA confirmed the carbonaceous nature of the PFA.

3.1.9. Metal extraction

Various extracting agents were used to examine their efficiency in the extraction of metals from the PFA. The extraction efficiencies of different extraction agents are summarized in Table 3.

When comparing the previous study (Al-Degs et al., 2014) with the current study, it was reported that a high percentage of metals extraction was achieved in an acidic solution (especially H_2SO_4). Using H_2SO_4, the percentages of metals extraction were 14.4% (for Cr) to 73.7% (for Mg) in the current study, while in previous studies, 13.3% (Cr) to 85.1% (Mg) were recorded. Furthermore, the elution of toxic metals to the environment was possible as mentioned from the previous analysis where all metals (except V) were easily leached using H_2O as an extracting agent (Al-Degs et al., 2014). This reflects that a good fraction of metals was weakly bonded to the PFA matrix. However, the poor extraction of V by H_2O and NaCl would be supported by its strong adherence to the PFA matrix. Moreover, the ethylenediaminetetraacetic acid (EDTA) was effective for metals elution with an extraction percentage ranging from 9.2% (for Cr) to 77.4% (for Mo). In contrast, NaOH was seen to be ineffective for metals extraction, which could be due to a high affinity between Mo and NaOH. After analyzing both studies, it could be concluded, that the extraction of metals is not a promising procedure for the PFA utilization. As indicated from the earlier analysis, V and Ni are the most abundant metals in the PFA with the content of 3.1 wt% and 0.71 wt%, respectively. From Table 3, the maximum extraction values were 15.6% for V and 55.6% for Ni using H_2SO_4. From an economical point of view, the earlier metal extraction values are low and indicated incomplete combustion, hence the removal of

Table 3
Metals extraction (wt%) from the PFA using different extracting agents.[a].

Extracting agent	wt% metals extraction						
	Ni	V	Mo	Cr	Zn	Cu	Mg
H_2SO_4	55.6	15.6	73.7	14.4	32.2	14.4	70.4
H_3PO_4	52.0	14.3	38.1	15.2	30.2	–	69.1
$(NH_4)_2SO_4$	33.4	<1	6.6	8.2	27.1	18.2	55.2
NH_4NO_3	21.0	<1	4.5	3.4	17.7	23.3	56.1
$NH_4O_2CCO_2H$	<1	<1	ND	3.3	2.1	ND	33.1

[a] The reported values were averaged of three identical trials (RSD < 4.4%) The "liquid to solid" "L/S" ratio was maintained at 50.0 cm^3/g, agitated for 24 h at 25 °C (±1 °C), and centrifuged (5000 rpm). ND: not detected.

these valuable metals using other extracting agents is required to obtain a complete combustion (Taggart et al., 2016). Moreover, two common tests were performed to assess whether the PFA is hazardous due to its toxicity, namely the toxicity characteristic leaching test (TCLP) and synthetic precipitation leaching procedure (SPLP). In both procedures, the PFA is agitated with a certain extraction agent with a mass ratio of 1:20 for 24 h and the leached metals are quantified in the final extract. For the TCLP, the employed extracting agent (0.1 M acetic acid) acted as municipal landfill leachate, while for the SPLP, 0.024 mM H_2SO_4 and 0.018 mM HNO_3 mixture was used as a simulation for acid-polluted rainwater. The concentration of the extracted metals for the TCLP was 53.0 mg/L, 0.13 mg/L, 0.51 mg/L, and 0.53 mg/L for Ni, Cr, Zn, and Cu, respectively. While for the SPLP test, the level of metals in the final extract was 40.6 mg/L, 0.25 mg/L, 0.42 mg/L, and 0.41 mg/L, respectively. According to the United States Environmental Protection Agency (USEPA), the concentration limits for Ni, Cr, Zn, and Cu in a leachate of a solid waste should not exceed 1.30 mg/L, 5.0 mg/L, 500 mg/L, and 100 mg/L, respectively. However, there are no regulated limits for V, Mo, and Mg metals (Mohajerani and Larobina, 2016). Based on the results in Table 3, the USEPA limits confirmed that the level of Ni is significantly higher, and this ash should not be directly discharged into the environment without special treatment. The levels of Zn and Cu are within the safe limits. The level of Cr is 4-times higher than the recommended limit. Even though not listed by the USEPA, the level of V in the final extract is extremely high 50.9 mg/L and 57.7 mg/L for the TCLP and the SPLP, respectively. Elimination of V and Ni from the ash is necessary before discharging PFA into the local environment.

3.2. Physical and chemical properties of prepared PFA based-geopolymer

Five GPs were prepared using different amounts of the PFA Table 4 summarizes the compositions of the prepared GPs and the PFA mixtures with their physical properties.

The density and thermal conductivity (T) of the prepared GPs were significantly affected by the amount of the PFA added. The density of the prepared GPs reduced from 1821 to 1201 kg/m^3. The density of the prepared GPs decreased by 8.0 wt%, 18.1 wt%, 25.5 wt %, and 34.0 wt% when 15 wt%, 26 wt%, 35 wt%, and 42 wt% PFA was incorporated. The large reduction in the GP5 could be due to the large volume occupied by the PFA. The GPs become more porous as the PFA amount increased. Low-density or lightweight materials are favorable in constructions because of its lower structural dead load, lower thermal conductivity, and lower transport costs. Lightweight building materials could be replaced with the standard materials. However, the materials of higher strength or materials of a particular look are still needed to be studied. A lightweight GP prepared by adding 42 wt% PFA (equivalent to 61% by vol.) could be utilized in various applications depending on the required strength.

The thermal conductivity of the prepared GPs is an important index for their application. The thermal conductivity of a material can be defined as the rate at which the material conducts heat. It measures the heat transfer in a material whereby a lower T value indicates better insulation. Geopolymer, in general, has a low T value of less than 0.70 W/mK, which is approximately 50% lower than Portland cement materials. Large amounts of heat loss from buildings are dependent on the thermal conductivity of the materials in the walls and roof (Mohajerani and Larobina, 2016). Mostly, the thermal conductivity is highly dependent on the porosity and density of the material. Building materials must prevent or reduce heat flow from one side to another. In this work, the following empirical equation (2) was applied for estimating the thermal conductivity of the prepared GPs (Lanzerstorfer, 2010; Al-Ghouti et al., 2011; Abdellatif, 2002):

$$T = 0.0559e^{(0.0014D)} \quad (2)$$

where T and D represent thermal conductivity and dry density of the material, respectively.

The earlier formula was developed using more than 250 experimental tests reported for various types of building materials including bricks, concrete, and aggregates. Equation (2) demonstrates a high coefficient of determination with an R^2 of 0.885. As can be noted from Table 4, it was observed the increase in the PFA percentage was inversely proportional to the thermal conductivity of the GP, as the percentage of PFA increases the thermal conductivity of GPs decreases. For instance, the addition of 42 wt% PFA reduced thermal conductivity by 57%, which is a substantial amount in terms of energy saving, which also show promising application in construction.

3.2.1. Mechanical properties and water absorption test for PFA based-geopolymer

Before discussing the physical and chemical results, it is important to calculate the following ratios of Si/Al, Na/Al, and H_2O/Al as they indicate the stability of the final GPs. Table 5 summarizes the ratios of the materials making up GPs along with the typical ratios for best GPs. The XRD analysis of the clay sample revealed that kaolinite (particle diameter 45 μm−63 μm) is the major mineral while smectite and quartz are present as minor minerals. The loss on ignition (LOI) was found to be 15.89. As indicated from the chemical analysis, the selected clay is a good starting material for preparing GPs where the total content of SiO_2 and Al_2O_3 is 68%, which is essential for preparing a well-structured 3D GPs. For obtaining a solid and a chemically stable GPs, the following ratios given in Table 5 should be within certain ranges as recommended in the literature (Hong et al., 2000; Dias-Ferreira et al., 2003; Vitolo et al., 2000). Accordingly, the PFA was added to the reaction mixture in different amounts while maintaining the earlier ratios within the recommended ranges.

Among the listed ratios, Si/Al is the most important one that should be adjusted to end up with a GP of high compressive strength even in the presence of carbonaceous FA. As seen in various studies, the Si/Al ratio should be 3:1 or at least within the range 1.5−2.5. Al-Ghouti et al. (2012b) studied the potential use of GP containing fly ash produced in heavy fuel power plants for toxic metal fixation. A local kaolinite was used in addition to fly ash and NaOH mixture; five GPs were prepared at the following ratios: Si/Al: 1.68−4.71, Na_2O/Al_2O_3: 1.48−1.84, Na/Al: 0.74−0.92.

As shown in Table 5, the ratio was around 4.0 in all GPs, which is higher than the recommended value (Al-Ghouti et al., 2012b; Al-Degs et al., 2014). Moreover, the GPs of high compressive strengths which have Si/Al ratios of 3.0 and 1.5. Na/Al and SiO_2/Al_2O_3 in the prepared GPs were within the typical ranges and many

Table 4
The compositions of the prepared GPs and the PFA mixtures with their physical properties.

Geopolymer (GP)	Kaolinite	PFA (g)[b]	PFA (wt%)	PFA (vol%)	Density (kg/m^3)	Thermal conductivity (W/m.k)
GP1	100	0	0	0	1821	0.70
GP2	100	25	15	20	1676	0.57
GP3	100	50	26	38	1491	0.44
GP4	100	75	35	50	1356	0.37
GP5	100	100	42	61	1201	0.30

Table 5
The ratios of the materials making up the GPs and the highest observed compressive strengths for the samples after 28 days of curing (Al-Degs et al., 2014).

GP[a]	Si/Al[a]	Na/Al[b]	H_2O/Na[c]	SiO_2/Al_2O_3[d]	Na_2O/Al_2O_3[e]	Compressive Strength (MPa)
GP1	4.12	1.25	2.02	3.32	0.98	33.0
GP2	4.11	1.20	2.12	3.31	0.94	22.4
GP3	4.10	1.15	2.24	3.29	0.91	10.2
GP4	4.07	1.16	2.37	3.28	0.85	10.6
GP5	4.06	1.03	2.52	3.27	0.81	5.2

Recommended ratio: a. 3:1, b. 1.0–1.29, c. 11–15, d. 3.0–3.8, and e. 1.0.

GPs were of similar ratios. The ratio that does not fall in the recommended range is H_2O/Na as the observed range was 2–2.5 while it should be within 11–15. This could explain the large reduction in compressive strength. Adding PFA to the reaction mixture (up to 100 g) has increased H_2O/Na value from 2.02 to 2.52, which is equivalent to a 23% increase. In this case, higher ratios of H_2O/Na would be simply achieved by increasing the amount of water and this was not followed due to its negative influence on geopolymerization reaction as the concentration of NaOH should be more than 12.0 M. In the current study, however, the molar concentration of NaOH was 16.6 M. Application of kaolinite for preparing stable and rigid GPs has been outlined in the literature (Galiano Luna et al., 2011).

Based on the compressive strength, density, and thermal conductivity values of prepared geopolymers, they could be classified into three Classes, namely Class I, Class II, and Class III. This functional classification was based on the International Union of Laboratories and Experts in Construction Materials, Systems, and Structures (RILEM). Class I is represented with a density of 1440–1840 kg/m^3, compressive strength greater than17 MPa, and T of 0.4–0.7 W/mK. Class II is denoted with a density of 800–1400 kg/m^3, the compressive strength of 3.4–17 MPa, and T of 0.22–0.43 W/mK. Class III is characterized by a low density (240–800 kg/m^3), compressive strength (0.7–3.4 MPa, and k (0.065–0.22 W/mK) (Jaya et al., 2020). Based on the values in Tables 4 and 5, (GP1 and GP2) and (GP4 and GP5) are classified as Class I and Class II, respectively. However, the GP3 is almost classified as Class II.

Based on the results of the bulk density, compressive strength, and thermal conductivity obtained for the metakaolin geopolymer by Jaya et al. (2020), the metakaolin geopolymer could be classified as Class II lightweight concrete for structural and insulating purposes according to the RILEM.

3.2.2. Compressive strength and water absorption tests for PFA based-geopolymer

The compressive strength test was carried out for the dry GP samples after 1, 7, 14, and 28 days of curing as recommended by ASTM (Huseien et al., 2016). Compressive strength and water absorption results are presented in Table 6.

The following conclusions can be deduced from Tables 6 and i) for the dry samples, all the prepared GPs displayed high compressive strength for longer curing times, which was caused by the hard matrix of the GP, formed over time. For the control sample GP1 (0 wt% PFA), the compressive strength increased from 27.3 MPa to 33.0 MPa from day1 and day28, respectively, ii) relatively speaking, the variation in compressive strength values over curing times was not high and this would be credited to the fast development of GPs matrix within the first 24 h of curing. In a similar study, a 77% reduction in compressive strength of a waste-rubber concrete (50 vol%) has been reported (Fattuhi and Clark, 1996). The results reported on dry GPs indicated that the mechanical strength got weaker as with the addition of the PFA which was observed at all curing times, iii) when compared with the control sample, the compressive strength has significantly been reduced from 27.3 MPa to 3.2 MPa which is equivalent to 88.3% reduction in compressive strength. The recommended limits for a lightweight construction material compressive strength are higher than 4.5 MPa and a dry density of less than 1500 kg/m^3 to get better thermal conductivity (Jeong et al., 2017). Accordingly, the prepared GPs met the requirement and are eligible to be used in the construction field. The reduction in compressive strength with the addition of the PFA would be attributed to the following reasons: at higher PFA mass percentage, the composite became lighter due to the formation of voids and porosity (compare to the control sample) making it a weak matrix; air-entrainment as the more the air to voids ratio, the lighter the matrix and lower compressive strength; and the nature of chemical interaction between the PFA and the GP materials. Similarly, Freire et al. (2020) investigated the application of FA based GP as an adsorbent and found that after 7 days of curing the compressive strength was 16.5 MPa and it decreased to 11 MPa after 28 days due to the microstructural reorganization, thus can be utilized as cement for CO_2 capture and storage.

Moreover, Nguyen et al. (2020) investigated the compressive strength of FA based GP concrete and found that it was in the range of 5.44 MPa–67.86 MPa. Another study determined the development of GP mortars from processes and unprocessed FA particles and results showed that the compressive strength after 28 curing days of the unprocessed FA was 12.12 MPa while the processed FA had a compressive strength of 18.12 MPa.

Furthermore, the water absorption properties of all specimens were improved by incorporating more PFA. This test was carried out to evaluate the water-permeable porosity of the geopolymer mortars. Increasing PFA from 0 to 61 vol% increased water absorption value from 6.6 wt% to 13.3 wt% for specimens collected after 28 days of curing which indicated water absorption capacity was doubled. Similar observations were noted for samples obtained other curing times (Day1, Day7, and Day14). The high-water absorption owed it to the high porosity of the materials that were

Table 6
The compressive strength and water absorption tests for the studied GPs.

Compressive Strength (MPa)				
GP	Day1	Day7	Day14	Day28
GP1	27.3	28.4	29.2	33.0
GP2	22.4	22.1	21.6	22.4
GP3	7.5	7.3	8.4	10.2
GP4	7.5	6.2	ND	10.6
GP5	3.2	3.4	4.6	5.2
Water Absorption (wt%)				
GP1	9.1	6.8	6.7	6.6
GP2	8.4	6.8	6.5	6.5
GP3	10.1	9.8	9.3	6.3
GP4	12.3	12.9	12.1	11.4
GP5	13.4	13.2	13.2	13.3

a The reported values were averaged of three tests on three specimens with RSD <10% compressive strength and RSD <12.3 for the water absorption test.

created by incorporating more amount of carbonaceous FA, which has a high affinity for water. However, a different trend was noted in the literature (Yu et al., 2015). While Fattuhi and Clark (1996) found more amounts of rubber waste to the cement particles adds up with concentrate of lower water absorption compared to the control sample. Various studies determined the water absorption percentage for different FA based GP. Masi et al. (2014) found that it was in the range of 24%–27%, Abdollahnejad et al. (2015) found that it was between 10% and 26%. Furthermore, Abdullah et al. (2012) mentioned that water absorption was in the range of 1.22%–2.35%. Similarly, Kumar and Ramamurthy (2017) found that the percentage was between 5 and 19 for FA based GP paste and 3 to 26 for FA based GP mortar.

3.2.3. Chemical stability of GPs: electrical conductivity, pH measurements, metals leaching

For more assessment of the matrix stability of the GPs, pH, and electrical conductivity measurements (over the period 1 h–24 h) were carried out for all samples including PFA, and the results are shown in Fig. 3.

From Fig. 3A, the pH plot displayed that the acid/base characteristics of the samples were different. The PFA was treated with an acidic solution (pH 2.8–3.3 over the tested period), while all GPs were treated with alkaline solutions. The acidic nature of the PFA could be due to the low content of strong alkaline oxides (like CaO) which were present in small amounts (0.8%). The pH plot indicates that the interaction of the PFA and the GPs with water is a fast process where pH values do not significantly change after 1.0 h of the interaction. An interesting point in the pH plot is that pH decreased with the amount of added PFA. For example, pH values obtained after 24 h were 10.65, 10.05, 9.56, 9.26, and 8.88 for GP1, GP2, GP3, GP4, and GP5, respectively.

On the other hand, the electrical conductivity plot indicated that the reported values for the ions leaching from the PFA and the GPs are extremely high. Moreover, the reported electrical conductivity of the samples is significantly high when compared to that of tap or well water (0.06–0.1 S/m). For all specimens, the lowest electrical conductivity was observed after 24 h and this would be attributed to the re-precipitation of soluble ions by OH^- ions, hence decreasing electrical conductivity. This was not observed in the PFA where the electrical conductivity value was always almost stable. It is interesting to notice that the electrical conductivity of the GPs increases with the amount of the PFA. This can be attributed to the weak chemical interaction between the PFA components and the aluminosilicate matrix and the presence of solubilizing ions (like chloride 0.65% in original PFA), which facilitate ions mobility cause to weaken the entire structure.

Two positive effects of using the alkaline solution (i.e. NaOH) in the geopolymerization process, namely the potential enhancement of the PFA interaction with the geopolymeric matrix, leading to improved mechanical and electrical properties, and the dispersion of PFA within the geopolymeric matrix, allowing the electrons to easily move within the matrix, resulting in an improved electrical conductivity; indicating the potential application of PFA-geopolymers as self-heating or damage sensing materials (Saafi et al., 2013).

As confirmed earlier, the prepared GPs displayed a degree of ions leaching with extremely high electrical conductivity values. Accordingly, it is also necessary to determine the nature of leached ions considering the toxicity of these ions in the PFA. Moreover, the structural elements (Si, Al, and Na) were also tested as the GPs and compressive strengths indicating the presence of these elements in the matrix. Synthetic precipitation leaching procedure (SPLP) was adopted for assessing the degree of metals leaching from the rigid GPs matrix. Table 7 summarizes the amounts of toxic metals leached from the GPs and the PFA as well.

Moreover, it was also found that the release of metals was dependent on the amount of the PFA added, as the increase in metal leaching is proportional to the amount of the PFA added. The high release of V and Ni from the GPs compared to other metals could be due to their high presence in the PFA and/or to unsuccessful participation in the polymerization process. The mechanisms of the metals leaching from the GPs were studied. It was concluded that for the optimal use, the GP1, GP2, and GP3 were the best materials to be used in construction materials were the level of leached metals is less than the regulated values set by the USEPA for solid wastes.

3.2.4. Potential applications of PFA

From the earlier physical and chemical tests, potential environmental and industrial management of the PFA could be determined. Since the ash consists of large amounts of valuable and toxic metals, it is vital to carry out leaching tests using various extracting agents to assess the degree of extractability of metals and hence their effect on the environment. The other main application of the PFA is in construction materials, which can be achieved by producing a construction material that consists of the ash while maintaining the needed physical and chemical proprieties (Yao et al., 2015). Application of the PFA as an adsorbent is also a potential application in which various studies showed the ability of an FA-geopolymer on the removal of various contaminants from the aqueous medium as shown in Fig. 4. This could only be confirmed after assessing the degree of leachability of toxic metals. Furthermore, according to Singh and Middendorf (2020), the removal of

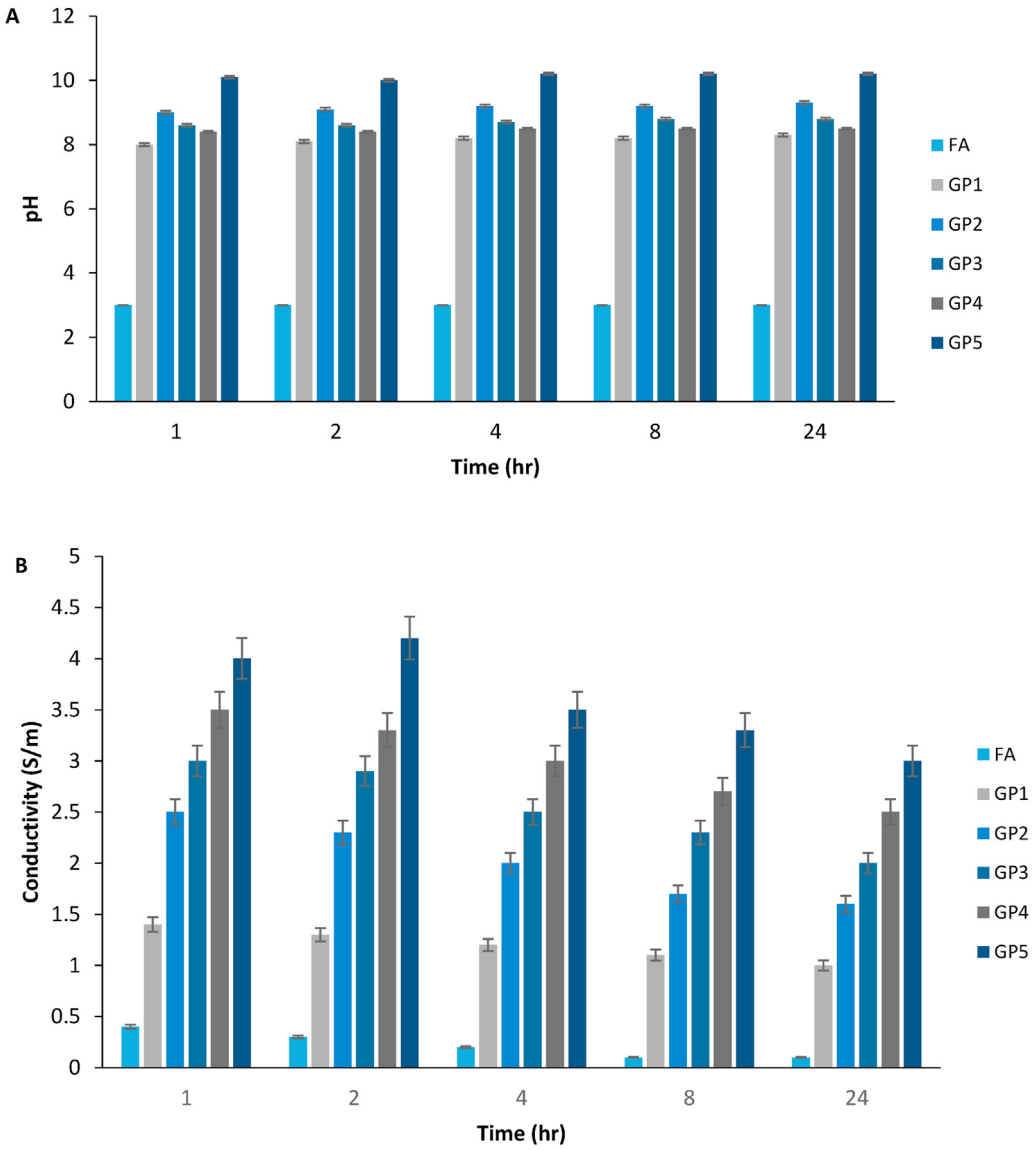

Fig. 3. (A) pH measurements and (B) electrical conductivity measurements of matrix stability of the PFA and the prepared geopolymers.

Table 7
Levels (mg/L) of released metals from the PFA and the prepared GPs. The values in the bracket are the limit values of the USEPA (Al-Degs et al., 2014).

Material	Ni (1.3 mg/L)	Cr (5.0 mg/L)	Zn (500 mg/L)	Cu (100 mg/L)	V
PFA	40.6	0.25	0.42	0.41	57.7
GP1	ND	ND	ND	ND	ND
GP2	0.81	ND	ND	ND	ND
GP3	1.21	ND	ND	ND	12.3
GP4	2.93	0.10	0.33	ND	22.4
GP5	8.62	0.15	0.36	ND	31.7

ND: Not Detectable.

dyes from sewage could be done by using GPs as adsorbents where different dyes adsorb in different ways. For instance, Li et al. (2006) found that adsorption of crystal violet is endothermic while methylene blue adsorption was exothermic. Moreover, it was found by Hashimoto et al. (2017) that FA-geopolymer paste products are highly resistant to H_2SO_4 solution at 60–220 °C and they are a good candidate as refractory material for oil refinery plants. Furthermore, various studies confirmed the possibility of using FA geopolymers as fire-resistant (Singh et al., 2015; Rashad, 2019; Zhang et al., 2014). Jiang et al. (2020a) studied the effect of temperature up to 1200 °C on the thermal and physical behavior of geopolymer concrete. The results showed its feasibility in fire-resistant building applications. Similarly, Jiang et al. (2020b) investigated the impact of 1200 °C on both Class C and Class F FA geopolymer. The results illustrated that the Class C FA geopolymer had better thermo-physical performance than the Class F FA geopolymer at temperatures higher than 800 °C.

Ordinary concrete can be replaced by GPs due to their similar mechanical properties as the normal Portland cement binders, with less CO_2 emissions. GPs have high thermal stability and corrosion resistance (Cai et al., 2020). Since FA contains silica and alumina in high percentages, it is considered as one of the most used solid precursors that are suitable to be utilized as a source material for GPs. Recently, FA of different origins have been added to building composites, primarily due to its lightweight characteristic and having similar chemical and physical characteristic as cement, and secondly due to its capability of reducing metal leaching. According to a study conducted by Bajpai et al. (2020) who investigated the

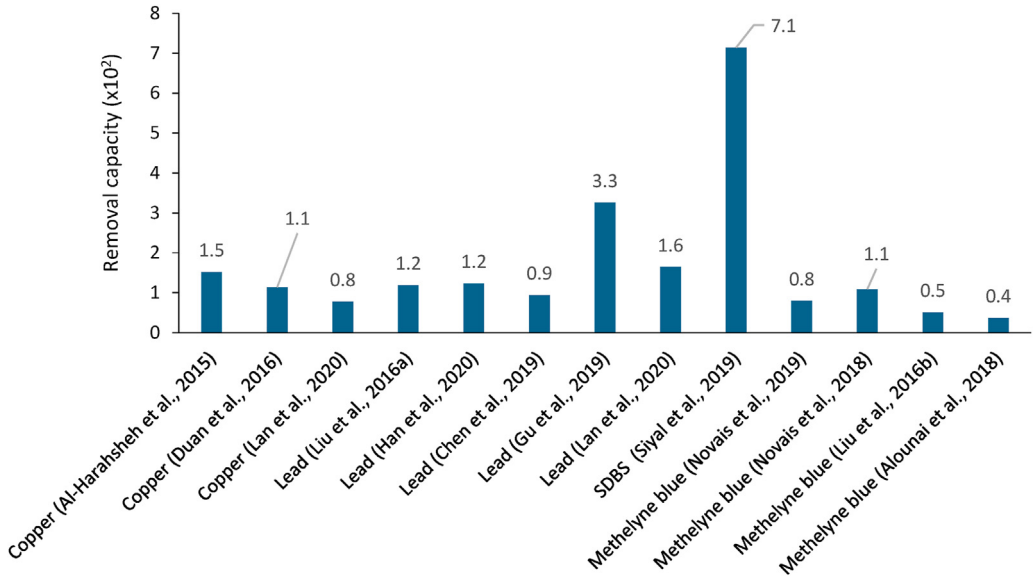

Fig. 4. Adsorption of different pollutants by FA-based geopolymer. *SDBS = sodium dodecylbenzene sulfonate. Al-Harahsheh et al., 2015, Chen et al., 2019, Duan et al., 2016, EL Alouani et al., 2018, Gu et al., 2019, Lan et al., 2020, Liu et al., 2016a, Liu et al., 2016b, Novais et al., 2018, Novais et al., 2019, Nunes and Guerreiro, 2011, Siyal et al., 2019.

durability of FA-geopolymer and kaolin FA-geopolymer, it was found that excellent durability and mechanical properties, were offered by FA-geopolymer concrete, are not obtained by the ordinary Portland cement concrete. Furthermore, the results illustrated that the overall performance of the FA-geopolymer had higher resistance to chemical attack than the ordinary Portland cement concrete. It was found that the use of FA-geopolymer concrete could reduce the cost by 10.87%–17.77% per unit volume.

Moreover, another study investigated the effect of alccofine on low-calcium FA-geopolymer concrete, results showed that the different percentages of alccofine can improve the fresh and hardened properties of low-calcium FA-geopolymer and it can be used for cast in situ practices at ambient temperature (Saloni et al., 2020). According to Tho-In et al. (2018), similar strengths and appearances were observed when compared to the mortars and concretes using FA-geopolymer binders to the normal Portland cement. In a recent study, Seto et al. (2017) investigated FA as a replacement of cement by developing a model containing 10%, 25%, and 50% of FA as cement. The result showed that FA was able to lower the environmental impact by 43%. On the other hand, Tosun-Felekoglu et al. (2017) investigated the sustainability of Class C and Class F FA in High Tenacity Ply propylene Engineered Cementitious composite application. It was concluded that the Class F ash demonstrated a reduction of up to 45% of the cost and 55%.

Moreover, it has been shown that adding FA generated in municipal wastewater into polymerization reaction forms a stable GP, which resists metals leaching and has a very stable structure with a compressive strength of 7 MPa. It is necessary to mention that PFA of high SiO_2 and Al_2O_3 contents are good starting materials for preparing solid materials via geopolymerization (Timakul et al., 2015). Moreover, PFA of particle diameter $\leq$45 μm is more favorable than coarser particles when preparing construction materials to maintain reasonable replacement of cement particles (Owaid et al., 2012). Large particles of the PFA are recommended as filters not in preparing normal cement concrete. Despite the addition of high Si and Al content is necessary, the application of PFA of high organic content (as the one described in this work) is not reported yet. As reported earlier, the AMD of FA is 70.2 μm and the content of SiO_2 and Al_2O_3 is not high, therefore, the application of this ash in geopolymerization is possible where trapping of ash particles within the 3D structure of the GP may reduce metals leaching.

4. Conclusions

The aim of this paper was to develop a PFA based-geopolymer with high compressive strength and water absorption and to determine the suitable application for the prepared GPs. From the obtained results, it can be concluded that the PFA can be used for the development of geopolymers that can be used in various applications as well as reducing the environmental concerns associated with the disposal of this waste. The following conclusions can be drawn:

- In comparison to coal fly ash, the PFA was found to have a low percentage of SiO_2 and Al_2O_3 due to the low Si and Al content in the feed fuel.
- Geopolymerization was possible, and five GPs with different amounts of PFA were prepared.
- Increasing the amount of the PFA in the GP improved the water absorption ability as it increased from 6.6 to 13.3 with increasing the PFA from 0 vol% to 61 vol% after 28 curing days.
- The PFA percentage and thermal conductivity are inversely proportional.
- The PFA has a carbonaceous nature, a high level of fixed carbon, high porosity with a total pore volume of 0.02 cm^3, and average pore width of 22.2 nm, as well as having a low bulk density of 0.381 g/mL.
- The prepared GP1, GP2, and GP3 could be useable in construction material with metal leachability less than the USEPA regulated values.

4.1. Practical implications

This article provides knowledge on the development of stable GPs using PFA with high compressive strength and water absorption to promote cleaner production, sustainability, and recycling of waste. With this article, investigators from around the world can understand the potential applications and environmental relevance of PFA. It was shown that the highest metal extraction percentage

was achieved in an acidic solution (especially H_2SO_4). It was also found that the release of metals was dependent on the amount of the PFA added, as the increase in metal leaching is proportional to the amount of the PFA added. Specifically, the metals leachability from the PFA using different extracting agents, namely H_2SO_4, H_3PO_4, $(NH_4)_2SO_4$, NH_4NO_3, and $NH_4O_2CCO_2H$ was also considered. Despite the addition of high Si and Al content is necessary, the application of PFA of high organic content (as the one described in this work) is not reported yet, therefore, the application of this ash in geopolymerization is possible where trapping of ash particles within the 3D structure of the GP may reduce metals leaching. In overall, it can be concluded that the PFA can be used for the development of a geopolymer that can be used in various applications as well as reducing the environmental concerns associated with the disposal of this waste.

4.2. Research limitations, and future research gap

Although efforts were done to carry out a comprehensive study on the development of stable GPs with high compressive strength and water absorption and determining the suitable application for the prepared GPs, the metal extraction from the PFA and the prepared GPs were limited to certain extracting agents; future research may be conducted in using more extracting agents, enhancement of geopolymer performance, and investigating the application of PFA based-geopolymers as adsorbents for the removal of metals and organic pollutants.

CRediT authorship contribution statement

Mohammad A. Al-Ghouti: Conceptualization, Supervision, Visualization, Methodology, Formal analysis, Validation, Investigation, Writing - review & editing. **Yahya S. Al-Degs:** Conceptualization, Supervision, Visualization, Methodology, Formal analysis, Validation, Investigation, Writing - review & editing. **Ayoup Ghrair:** Methodology, Formal analysis, Validation, Investigation, Writing - review & editing. **Mahmoud Ziedan:** Methodology, Formal analysis, Validation, Investigation, Writing - review & editing. **Hani Khoury:** Methodology, Formal analysis, Validation, Investigation, Writing - review & editing. **Jafar I. Abdelghani:** Writing - review & editing. **Majeda Khraisheh:** Writing - review & editing.

Declaration of competing interest

The authors declare that they have no known competing financial interests or personal relationships that could have appeared to influence the work reported in this paper.

Acknowledgement

The authors are thankful for The Higher Council for Science and Technology, Jordan for the financial support. The findings achieved herein are solely the responsibility of the authors. Special thanks to Ms. Dana Da'na in helping with the final edits of the manuscript.

References

Abdel-latif, M.A., 2002. Recovery of vanadium and nickel from petroleum flyash. Miner. Eng. 15 (11), 953–961.
Abdollahnejad, Z., Pacheco-Torgal, F., Félix, T., Tahri, W., Barroso Aguiar, J., 2015. Mix design, properties and cost analysis of fly ash-based geopolymer foam. Construct. Build. Mater. 80, 18–30.
Abdullah, M., Hussin, K., Bnhussain, M., Ismail, K., Yahya, Z., Abdul Razak, R., 2012. Fly ash-based geopolymer lightweight concrete using foaming agent. Int. J. Mol. Sci. 13 (6), 7186–7198.
Ahmaruzzaman, M., 2010. A review on the utilization of fly ash. Prog. Energy Combust. Sci. 36 (3), 327–363.
Al-Degs, Y.S., Ghrir, A., Khoury, H., Walker, G.M., Sunjuk, M., Al-Ghouti, M.A., 2014. Characterization and utilization of fly ash of heavy fuel oil generated in power stations. Fuel Process. Technol. 123, 41–46.
Al-Ghouti, M.A., Al-Degs, Y.S., Ghrair, A., Khousry, H., Ziedan, M., 2011. Extraction and separation of vanadium and nickel from fly ash produced in heavy fuel power plants. Chem. Eng. J. 173 (1), 191–197.
Al-Ghouti, M.A., Ghrair, A., Khousry, H., Al-Degs, Y.S., Khraisheh, M., 2012a. Fly ash generated from heavy fuel incineration in power plants: physical and chemical characteristics. Indian J. Environ. Sci. 7 (11), 406–412.
Al-Ghouti, M.A., Al-Degs, Y.S., Ghrair, A., Khoury, H., Ziedan, M., 2012b. The potential use of geopolymer containing fly ash produced in heavy fuel power plants for toxic metals fixation: chemical and physical characteristics. Indian J. Environ. Sci. 7 (3), 84–92.
Al-Harahsheh, M., Al Zboon, K., Al-Makhadmeh, L., Hararah, M., Mahasneh, M., 2015. Fly ash based geopolymer for heavy metal removal: a case study on copper removal. J. Environ. Chem. Eng. 3 (3), 1669–1677.
Assi, L., Carter, K., Deaver, E., Anay, R., Ziehl, P., 2018. Sustainable concrete: building a greener future. J. Clean. Prod. 198, 1641–1651.
Bajpai, R., Choudhary, K., Srivastava, A., Sangwan, K.S., Singh, M., 2020. Environmental impact assessment of fly ash and silica fume based geopolymer concrete. Journal of Cleaner. Production 254, 120147.
Blissett, R., Rowson, N.A., 2012. A review of the multi-component utilization of coal fly ash. Fuel 97, 1–23.
Bohra, V., Nerella, R., Madduru, S., 2019. Material properties, processing & characterization of fly ash based geopolymer. Mater. Today Proc. 19 (6), 2617–2621.
Bray, D.J., Gilmour, S.G., Guild, F.J., Taylor, A.C., 2013. The effects of particle morphology on the analysis of discrete particle dispersion using delaunay tessellation. Compos. Part A Appl. Sci. Manuf. 54, 37–45.
Cai, J., Pan, J., Li, X., Tan, J., Li, J., 2020. Electrical resistivity of fly ash and metakaolin based geopolymers. Construct. Build. Mater. 234, 117868.
Chen, W., Lu, Z., Xiao, B., Gu, P., Yao, W., Xing, J., et al., 2019. Enhanced removal of lead ions from aqueous solution by iron oxide nanomaterials with cobalt and nickel doping. J. Clean. Prod. 211, 1250–1258.
Dias-Ferreira, C., Ribeiro, A.B., Ottosen, L.M., 2003. Heavy metals in MSW incineration fly ashes. J. Phys. IV 107 (463).
Duan, P., Yan, C., Zhou, W., Ren, D., 2016. Development of fly ash and iron ore tailing based porous geopolymer for removal of Cu(II) from wastewater. Ceram. Int. 42 (12), 13507–13518.
El Alouani, M., Alehyen, S., El Achouri, M., Taibi, M., 2018. Removal of cationic dye – methylene blue - from aque ous solution by adsorption on fly ash - based geopolymer. J. Mater. Environ. Sci. 9 (1), 32–46.
Fattuhi, N.I., Clark, L.A., 1996. Cement-based materials containing shredded scrap truck tyre rubber. Construct. Build. Mater. 10 (4), 229–236.
Foret, G., Bergametti, G., Dulac, F., Menut, L., 2006. An optimized particle size bin scheme for modeling mineral dust aerosol. J. Geophys. Res. 111 (17).
Freire, A., Moura-Nickel, C., Scaratti, G., De Rossi, A., Araújo, M., De Noni Júnior, A., et al., 2020. Geopolymers produced with fly ash and rice husk ash applied to CO2 capture. J. Clean. Prod. 273, 122917.
Galiano Luna, Y., Fernández Pereira, C., Vale, J., 2011. Stabilization/solidification of a municipal solid waste incineration residue using fly ash-based geopolymers. J. Hazard Mater. 18 (1), 373–381.
Gisi, S.D., Lofrano, G., Grassi, M., Notarnicola, M., 2016. Characteristics and adsorption capacities of low-cost sorbents for wastewater treatment: a review. Sustain. Mater. Technol. 9, 10–40.
Gu, P., Zhang, S., Zhang, C., Wang, X., Khan, A., Wen, T., et al., 2019. Two-dimensional MAX-derived titanate nanostructures for efficient removal of Pb(ii). Dalton Trans. 48 (6), 2100–2107.
Han, L., Wang, J., Liu, Z., Zhang, Y., Jin, Y., Li, J., Wang, D., 2020. Synthesis of fly ash-based self-supported zeolites foam geopolymer via saturated steam treatment. J. Hazard Mater. 393, 122468.
Hashimoto, S., Machino, T., Ando, K., Daiko, Y., Honda, S., Iwamoto, Y., 2017. Hot sulfuric acid-resistance of fly-ash-based geopolymer paste product due to the precipitation of natroalunite crystals. Construct. Build. Mater. 151 (1), 714–719.
Hong, K.J., Tokunaga, S., Ishigami, Y., Kajiuchi, T., 2000. Extraction of heavy metals from MSW incinerator fly ash using saponins. Chemosphere 41 (3), 345–352, 2000.
Hossaini, M., Aarabi, H., Bidi, A., Mohammadkhani, M., 2015. Construction and properties of Al/SiC composites using nano silicon carbide by powder metallurgy technique in pure aluminum alloy. Int. J. Sci. Eng. Res. 6, 801–811.
Huseien, G.F., Mirza, J., Ismail, M., Ghoshal, S.K., Ariffin, M.A., 2016. Effect of metakaolin replaced granulated blast furnace slag on fresh and early strength properties of geopolymer mortar. Ain Shams Eng. J.
Hu, W., Nie, Q., Huang, B., Shu, X., He, Q., 2018. Mechanical and microstructural characterization of geopolymers derived from red mud and fly ashes. J. Clean. Prod. 186, 799–806.
Jaya, N.A., Yun-Ming, L., Cheng-Yong, H., Al Bakri, A.M.M., Hussin, K., 2020. Correlation between pore structure, compressive strength and thermal conductivity of porous metakaolin geopolymer. Construct. Build. Mater. 247, 118641.
Jeong, Y., Koh, T., Youm, K., Moon, J., 2017. Experimental evaluation of thermal performance and durability of thermally-enhanced concretes. Appl. Sci. 7 (8), 811.
Jiang, X., Xiao, R., Zhang, M., Hu, W., Bai, Y., Huang, B., 2020a. A laboratory investigation of steel to fly ash-based geopolymer paste bonding behavior after exposure to elevated temperatures. Construct. Build. Mater. 254, 119267.
Jiang, X., Zhang, Y., Xiao, R., Polaczyk, P., Zhang, M., Hu, W., et al., 2020b.

A comparative study on geopolymers synthesized by different classes of fly ash after exposure to elevated temperatures. J. Clean. Prod. 270, 122500.
Jones, M.R., Sear, L.K.A., McCarthy, M.J., Dhir, R.K., 2006. Changes in Coal Fired Power Station Fly Ash: Recent Experiences and Use in Concrete. The UK Quality Ash Association (UKQAA).
Khan, H., Castel, A., Khan, M., 2020a. Corrosion investigation of fly ash based geopolymer mortar in natural sewer environment and sulphuric acid solution. Corrosion Sci. 168, 108586.
Khan, S., Zhang, Y., Kumar, Anil, Zavadskas, E., Sterimikiene, D., 2020b. Measuring the impact of renewable energy, public health expenditure, logistics, and environmental performance on sustainable economic growth. J. Sustain. Dev. 28 (4), 833–843.
Khan, S., Jian, C., Zhang, Y., Golpîra, H., Kumar, A., Sharif, A., 2019. Environmental, social and economic growth indicators spur logistics performance: from the perspective of South Asian Association for Regional Cooperation countries. J. Clean. Prod. 214, 1011–1023.
Khan, S., Sharif, A., Golpîra, H., Kumar, A., 2019. A green ideology in Asian emerging economies: from environmental policy and sustainable development. Sustain. Dev. 27, 1063–1075.
Kim, B., Prezzi, M., 2008. Evaluation of the mechanical properties of class-F fly ash. Waste Manag. 28 (3), 649–659.
Komnitsas, K., Zaharaki, D., 2007. Geopolymerization: a review and prospects for the minerals industry. Miner. Eng. 20 (14), 1261–1277.
Kröppl, M., Muñoz, I.L., Zeiner, M., 2011. Trace elemental characterization of fly ash. Toxicol. Environ. Chem. 93 (5), 886–894.
Kumar, E., Ramamurthy, K., 2017. Influence of production on the strength, density and water absorption of aerated geopolymer paste and mortar using Class F fly ash. Construct. Build. Mater. 156, 1137–1149.
Lanzerstorfer, C., 2010. Pre-processing of coal combustion fly ash by classification for enrichment of rare earth elements. Energy Rep. 4, 660–663.
Lan, T., Guo, S., Li, X., Guo, J., Bai, T., Zhao, Q., et al., 2020. Mixed precursor geopolymer synthesis for removal of Pb(II) and Cd(II). Mater. Lett. 274, 127977.
Liu, Y., Yan, C., Zhang, Z., Gong, Y., Wang, H., Qiu, X., 2016a. A facile method for preparation of floatable and permeable fly ash-based geopolymer block. Mater. Lett. 185, 370–373.
Liu, Y., Yan, C., Zhang, Z., Wang, H., Zhou, S., Zhou, W., 2016b. A comparative study on fly ash, geopolymer and faujasite block for Pb removal from aqueous solution. Fuel 185, 181–189.
Li, L., Wang, S., Zhu, Z., 2006. Geopolymeric adsorbents from fly ash for dye removal from aqueous solution. J. Colloid Interface Sci. 300 (1), 52–59.
Li, Z., Wang, L., Ma, G., 2020. Mechanical improvement of continuous steel microcable reinforced geopolymer composites for 3D printing subjected to different loading conditions. Compos. B Eng. 187, 107796.
Ma, G., Li, Z., Wang, L., Bai, G., 2019. Micro-cable reinforced geopolymer composite for extrusion-based 3D printing. Mater. Lett. 235, 144–147.
Masi, G., Rickard, W., Vickers, L., Bignozzi, M., van Riessen, A., 2014. A comparison between different foaming methods for the synthesis of light weight geopolymers. Ceram. Int. 40 (9), 13891–13902.
Mohajerani, A.K., Larobina, A.A.L., 2016. A practical proposal for solving the world's cigarette butt problem: recycling in fired clay bricks. Waste Manag. 52, 228–244.
Munawer, M., 2018. Human health and environmental impacts of coal combustion and post-combustion wastes. J. Sustain. Min. 17 (2), 87–96.
Nguyen, K., Nguyen, Q., Le, T., Shin, J., Lee, K., 2020. Analyzing the compressive strength of green fly ash based geopolymer concrete using experiment and machine learning approaches. Construct. Build. Mater. 247, 118581.
Novais, R., Ascensão, G., Tobaldi, D., Seabra, M., Labrincha, J., 2018. Biomass fly ash geopolymer monoliths for effective methylene blue removal from wastewaters. J. Clean. Prod. 171, 783–794.
Novais, R., Carvalheiras, J., Tobaldi, D., Seabra, M., Pullar, R., Labrincha, J., 2019. Synthesis of porous biomass fly ash-based geopolymer spheres for efficient removal of methylene blue from wastewaters. J. Clean. Prod. 207, 350–362.
Nunes, C.A., Guerreiro, M.C., 2011. Estimation of surface area and pore volume of activated carbons by methylene blue and iodine numbers. Quim. Nova 34 (3), 472–476.
Owaid, H.M., Hamid, R.B., Taha, M.R., 2012. A review of sustainable supplementary cementitious materials as an alternative to all-portland cement mortar and concrete. Aust. J. Basic Appl. Sci. 6 (9), 303–2887.
Pilehvar, S., Cao, V.D., Szczotok, A.M., Carmona, M., Valentini, L., Lanzón, M., Kjøniksen, A., 2018. Physical and mechanical properties of fly ash and slag geopolymer concrete containing different types of micro-encapsulated phase change materials. Construct. Build. Mater. 173, 28–39.
Pires, M., Querol, X., 2004. Characterization of candiota (south Brazil) coal and combustion by-product. Int. J. Coal Geol. 60 (1), 57–72.
Rashad, A., 2019. Insulating and fire-resistant behaviour of metakaolin and fly ash geopolymer mortars. Proc. Inst. Civ. Eng. Construct. Mater. 172 (1), 37–44.
Saafi, M., Andrew, K., Tang, P.L., McGhon, D., Taylor, S., Rahman, M., Yang, S., Zhou, X., 2013. Multifunctional properties of carbon nanotube/fly ash geopolymeric nanocomposites. Construct. Build. Mater. 49, 46–55.
Saloni, A., Singh, A., Sandhu, V., Jatin, J., Parveen, P., 2020. Effects of alccofine and curing conditions on properties of low calcium fly ash-based geopolymer concrete. Mater. Today Proc.
Seto, K.E., Churchill, C.J., Panesar, D.K., 2017. Influence of fly ash allocation approaches on the life cycle assessment of cement-based materials. J. Clean. Prod. 157.
Shang, J., Dai, J., Zhao, T., Guo, S., Zhang, P., Mu, B., 2018. Alternation of traditional cement mortars using fly ash-based geopolymer mortars modified by slag. J. Clean. Prod. 203, 746–756.
Shirai, H., Ikeda, M., Tanno, K., 2011. Factors affecting the density and specific surface area (blaine value) of fly ash from pulverized coal combustion. Energy Fuel. 25 (12), 5700–5706.
Shon, C., Sarkar, S.L., Zollinger, D.G., 2004. Testing the effectiveness of class C and class F fly ash in controlling expansion due to alkali-silica reaction using modified ASTM C 1260 test method. J. Mater. Civ. Eng. 16 (1), 20–27.
Sing, K., 2001. The use of nitrogen adsorption for the characterization of porous materials. Colloid. Surface. Physicochem. Eng. Aspect. 187–188, 3–9.
Singh, B., Ishwarya, G., Gupta, M., Bhattacharyya, S., 2015. Geopolymer concrete: a review of some recent developments. Construct. Build. Mater. 85, 78–90.
Singh, N.B., Middendorf, B., 2020. Geopolymers as an alternative to Portland cement: an overview. Construct. Build. Mater. 237, 117455.
Siyal, A., Shamsuddin, M., Rabat, N., Zulfiqar, M., Man, Z., Low, A., 2019. Fly ash based geopolymer for the adsorption of anionic surfactant from aqueous solution. J. Clean. Prod. 229, 232–243.
Taggart, R.K., Hower, J.C., Dwyer, G.S., Hsu-Kim, H., 2016. Trends in the rare-earth element content of U.S.-Based coal combustion fly ashes. Environ. Sci. Technol. 50 (11), 5919–5926.
Tan, T., Mo, K., Ling, T., Lai, S., 2020. Current development of geopolymer as alternative adsorbent for heavy metal removal. Environ. Technol. Innovat. 18, 100684.
Tho-In, T., Sata, V., Boonserm, K., Chindaprasirt, P., 2018. Compressive strength and microstructure analysis of geopolymer paste using waste glass powder and fly ash. J. Clean. Prod. 172, 2892–2898.
Timakul, P., Thanaphatwetphisit, K., Aungkavattana, P., 2015. Effect of silica to alumina ratio on the compressive strength of class C fly ash-based geopolymers. Key Eng. Mater. 659, 80–84.
Tiwari, M., Bajpai, S., Dewanga, U.K., Tamrakar, R., 2015. Suitability of leaching test methods for fly ash and slag: a review. J. Radiat. Res. Appl. Sci. 8 (4), 523–537.
Tosun-Felekoglu, K., Godek, E., Keskinates, M., 2017. Utilization and selection of proper fly ash in cost effective green HTPP-ECC design. J. Clean. Prod. 149, 2017.
Uzzal Hossain, M., Poon, C., Dong, Y., Xuan, D., 2018. Evaluation of environmental impact distribution methods for supplementary cementitious materials. Renew. Sustain. Energy Rev. 82, 597–608.
Vassilev, S.V., Vassileva, C.G., 2005. Methods for characterization of composition of fly ashes from coal-fired power Stations: A critical overview. Energy Fuel. 19 (3), 1084–1098.
Vitolo, S., Maurizia, S., Filippi, S., Brocchini, C., 2000. Recovery of vanadium from heavy oil and orimulsion fly ashes. Hydrometallurgy 57 (2), 141–149.
Wattimena, O., Antoni, A., Hardjito, D., 2017. A review on the effect of fly ash characteristics and their variations on the synthesis of fly ash based geopolymer. AIP Conf. Proc. 1887, 020041.
Yao, Z.T., Ji, S.X., Sarker, P.K., Tang, J.H., Ge, L.Q., Xia, M.S., Xi, Y.Q., 2015. A comprehensive review on the applications of coal fly ash. Earth Sci. Rev. 141, 105–121, 2015.
Yunusa, I.A.M., Loganathan, P., Nissanka, S.P., Manoharan, V., Burchett, M.D., Skilbeck, C.G., Eamus, D., 2012. Application of coal fly ash in agriculture: a strategic perspective. Crit. Rev. Environ. Sci. Technol. 42 (6), 559–600.
Yu, S., Tan, H., Wang, J., Liu, X., Zhou, K., 2015. High porosity supermacroporous polystyrene materials with excellent oil–water separation and gas permeability properties. ACS Appl. Mater. Interfaces 7 (12), 6745–6753.
Zhang, H., Kodur, V., Qi, S., Cao, L., Wu, B., 2014. Development of metakaolin–fly ash based geopolymers for fire resistance applications. Construct. Build. Mater. 55, 38–45.
Zhao, X., Liu, C., Zuo, L., Wang, L., Zhu, Q., Liu, Y., Zhou, B., 2020. Synthesis and characterization of fly ash geopolymer paste for goaf backfill: reuse of soda residue. J. Clean. Prod. 260, 121045.
Zhao, X., Liu, C., Wang, L., Zuo, L., Zhu, Q., Ma, W., 2019. Physical and mechanical properties and micro characteristics of fly ash-based geopolymers incorporating soda residue. Cement Concr. Compos. 98, 125–136.
Zhou, B.Y., Wang, L., Ma, G.W., Zhao, X., Zhao, X.H., 2019. Preparation and properties of bio-geopolymer composites with waste cotton stalk materials. J. Clean. Prod. 245, 118842.
Zhuang, X., Chen, L., Komarneni, S., Zhou, C., Tong, D., Yang, H., Yu, W., Wang, H., 2016. Fly ash-based geopolymer: clean production, properties and applications. J. Clean. Prod. 125, 253–267.